



# The Toulouse–Kleiman homotopic classification of topological defects in ordered systems illustrated by experiments

Pawel Pieranski, Maria Helena Godinho

## ► To cite this version:

Pawel Pieranski, Maria Helena Godinho. The Toulouse–Kleiman homotopic classification of topological defects in ordered systems illustrated by experiments. *Comptes Rendus. Physique*, 2024, 25 (G1), pp.367-388. <10.5802/crphys.206>. <hal-04628190>

**HAL Id: hal-04628190**

**<https://hal.science/hal-04628190v1>**

Submitted on 28 Jun 2024

**HAL** is a multi-disciplinary open access archive for the deposit and dissemination of scientific research documents, whether they are published or not. The documents may come from teaching and research institutions in France or abroad, or from public or private research centers.

L'archive ouverte pluridisciplinaire **HAL**, est destinée au dépôt et à la diffusion de documents scientifiques de niveau recherche, publiés ou non, émanant des établissements d'enseignement et de recherche français ou étrangers, des laboratoires publics ou privés.



HAL Authorization

# Distorsions with double topological character

## *Distorsions avec un caractère topologique double*

Pawel Pieranski<sup>✉,\*,a</sup> and Maria Helena Godinho<sup>✉,b</sup>

<sup>a</sup> Laboratoire de Physique des Solides, Université Paris-Saclay, Orsay, France

<sup>b</sup> i3N/CENIMAT, Department of Materials Science, NOVA School of Science and Technology, NOVA University Lisbon, Campus de Caparica, Caparica 2829 - 516, Portugal

E-mails: pawel.pieranski@u-psud.fr (P. Pieranski), mhg@fct.unl.pt (M.H. Godinho)

**Abstract.** We report here on recent experiments with linear topological defects, disclinations in nematics and dislocations in cholesterics, with the aim to illustrate the classification of defects in ordered media based on the homotopy theory conceived by Gérard Toulouse and Maurice Kléman. We focus on objects with double topological character : knotted and linked dislocations in cholesterics. Beside the "*double et tripple anneau*" Hopf links, considered by Toulouse et al., we report on experiments with their generalised version: necklaces made of minimal dislocation loops tethered on cargo dislocations.

**Résumé.** Nous rendons compte des expériences récentes réalisées avec les défauts topologiques linéaires: disinclinaisons dans les nématiques et les dislocations dans les cholestériques. Notre but est d'illustrer la classification de défauts dans les milieux ordonnés conçue par Gérard Toulouse et Maurice Kléman, basée sur la théorie de homotopie. Notre attention se porte sur les objets ayant un caractère topologique double: noeuds et liens faits de dislocations dans les cholestériques. Après les distorsions en "*double et triple anneau*", équivalents aux liens de Hopf, considérées par Toulouse et al., nous invoquons aussi les expériences avec leur version généralisée: colliers faits de dislocations en anneau enfilés sur une dislocation porteuse.

**Keywords.** topological defects, dislocations, knots, links, tangles.

**Electronic supplementary material.** Supplementary material for this article is supplied as a separate archive available from the journal's website under article's URL or from the author.

### 1. The birth of a new concept: classification of topological defects in ordered media

The article untitled "Principles of a classification of defects in ordered media" cosigned by Gerard Toulouse and Maurice Kleman [1] is a temporal mile-stone marking the birth of the unifying concept of "topological defects" that crowned the stay of Gerard Toulouse at the Laboratoire de Physique des Solides (LPS) in Orsay.

This birth was the result of fertile interactions between Toulouse and Kleman in a laboratory renown among others to studies of defects in condensed matter systems such as dislocations in solid crystals (Jacques Friedel [2,3]), vortices in superconductors and superfluids (Pierre-Gilles de Gennes [4,5]) or domain walls and singular points in magnets (Maurice Kleman). This diversity of defects in systems equipped with different order parameters increased considerably since 1969

---

\* Corresponding author.

when several young teams started to work on liquid crystals (headed by G. Durand, E. Guyon, M. Kleman, M. Veyssie). The liquid crystalline states of matter being liquid in three (nematics, cholesterics), two (smectics), or one (columnar) dimensions, are fragile and therefore frequently full of defects, such as disclinations and dislocations. Indeed, these defects are extremely easy to generate by phase transitions, flows or elastic strains. One could even say that the issue is not "how to generate them" but "how to get ride" of them. Moreover they are easy to observe in an optical microscope.

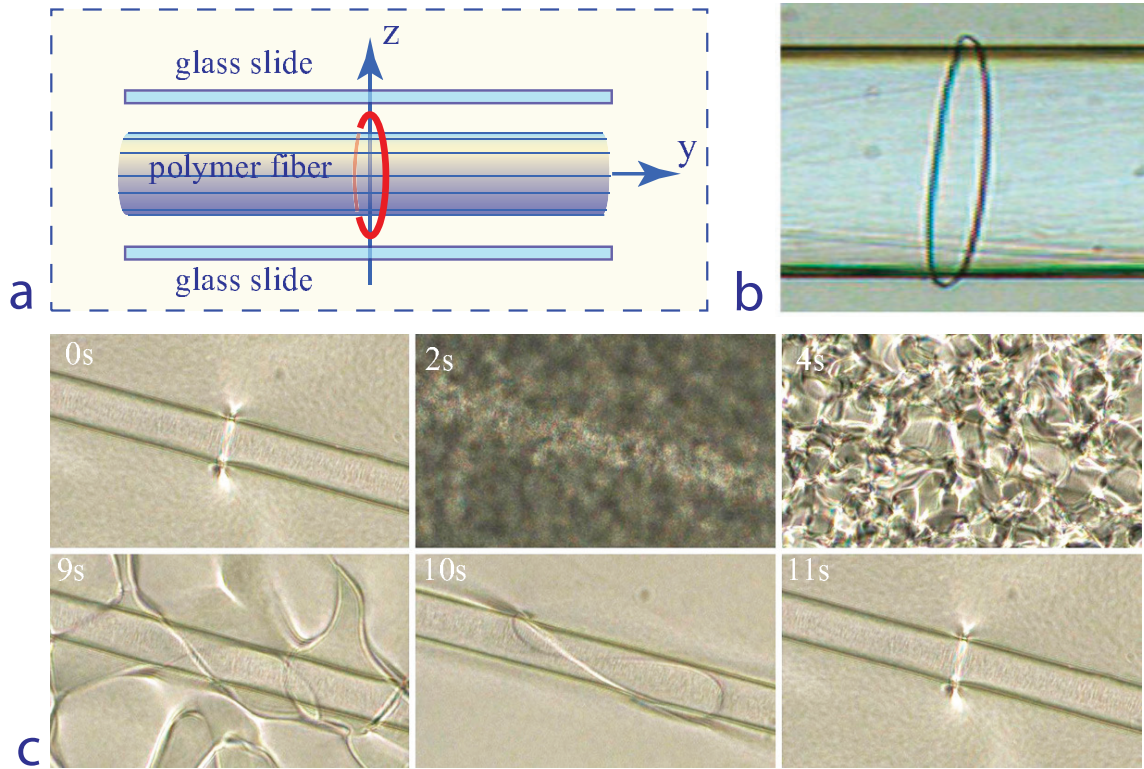


**Figure 1.** Experiment with a disclination loop tethered on a fiber. a) Geometry of the experiment. b) View of the tethered loop at equilibrium. c) Stretching of the loop by a turbulent flow and relaxation to the equilibrium.

Maurice Kleman, who worked previously on domain walls in magnets, started in 1969 to investigate intensively defects in liquid crystals with his students and visitors as well as in collaboration with other members of LPS and in particular with Gerard Toulouse.

In this favourable ambience, Toulouse and Kleman, who both had predilection for the mathematical abstraction, succumbed, fortunately, to it and embraced in one single glance the whole wide panorama of topological defects in condensed matter [1].

As a PhD student, one of the authors (P.P.) had the chance to listen to the wonderful lectures of Toulouse on topology in mathematics and physics illustrated by beautiful drawings made simultaneously with chalk on a black-board. Today we know that we had the privilege to hear Toulouse speaking about a new concept *in statu nascendi*. His explanations of classification of topological defects in condensed matter based on homotopy theory were crystal-clear.

Our aim here will be not to present this theory in details because today it is widely known (see f.ex. the book of Kleman and Levrentovich [6], the excellent review papers of Kurik and Lavrentovich [7] and of Smalyukh [8]). Instead of that we show how results of a few recent experiments can be interpreted in terms of it.

## 2. Captive $\pi$ disclinations in nematics

### 2.1. Experiment

The first experiment deals with the so-called "captive disclination loops" [9]. Its principle is represented schematically in Figure 1a where a disclination loop, the red circle, is tethered on a polymer fiber immersed in a nematic liquid crystal contained between two parallel glass slides.

Surfaces of the slides, coated with lecithin, orient the molecules of the nematic in the direction  $z$  perpendicular to them (homeotropic anchoring). The surface of the polymer fiber (a nylon fishing line) orients the nematic molecules in the direction  $y$  parallel to it (planar anchoring).

This disclination loop observed with a microscope (in transmitted light) from the  $z$  direction appears as a black line in Figure 1b. As we will see in the next section, it corresponds to a linear singularity of the molecular orientations which are usually represented by a unitary field  $\mathbf{n}$ , called director, locally parallel to the molecules. This linear singularity of the director field results in a singularity of the refractive index. Therefore, the disclination refracts the light so much that it appears in transmitted light as the black line.

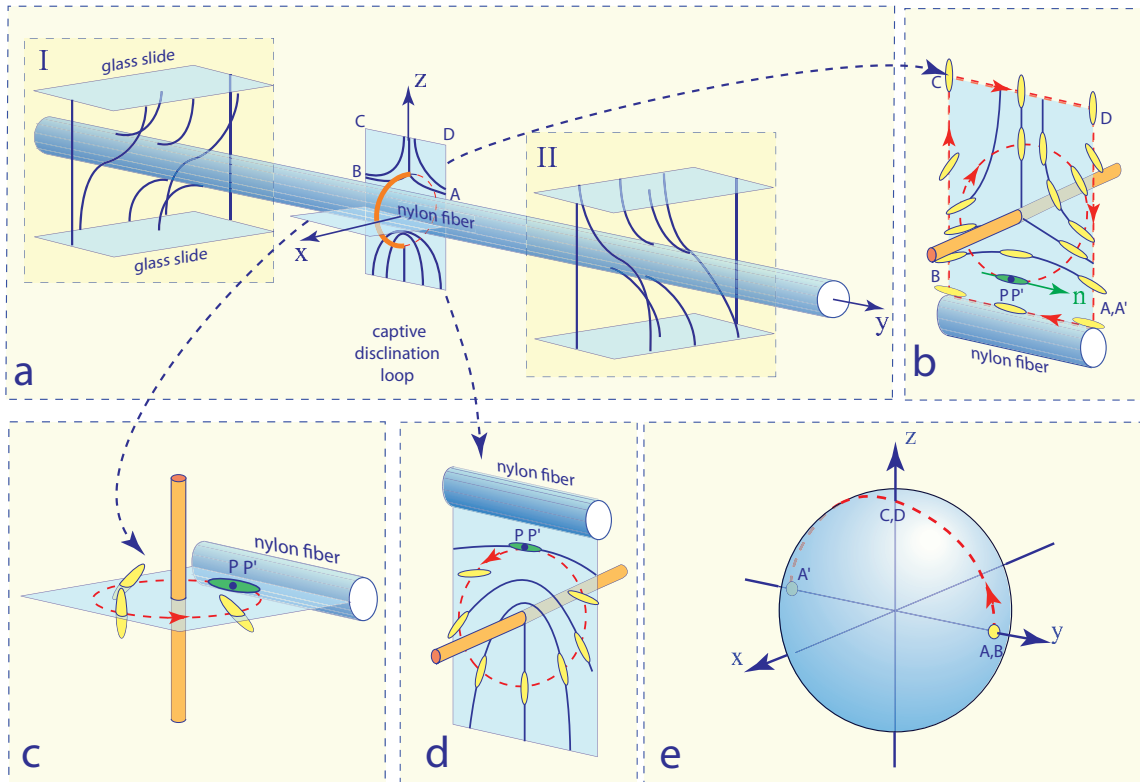


**Figure 2.** Analysis of the tethered disclination loop in terms of the homotopy theory. a) Perspective view of the director field. b-d) Director field in the vicinity of the disclination. e) Mapping of the director field from the closed trajectories in real space onto the unit sphere

The series of six pictures in Figure 1c shows that this captive disclination loop cannot be removed from the fiber by breaking it. This does not mean that it is very strong. On the contrary, it is elastically resilient. The second picture labelled "2s" shows that the turbulent flows, due to an electrohydrodynamic instability, stretched and entangled this disclination loop so much that

it "almost filled the whole volume" of the nematic. For this reason in the picture labeled "2s" the sample appears as turbid (almost black) - the illuminating light beam is almost completely diffused by the stretched and entangled disclination loop. The next four pictures show that once the turbulent flow is switched off, the disclination recovers in a few seconds its initial length, shape and position due to the orientational elasticity of nematics, and which is the most important: it remains tethered on the polymer fiber.

## 2.2. Interpretation in terms of the homotopy theory

Let us interpret now results of this simple experiment in terms of the theory proposed by Toulouse and Kleman. To start with, let us remind that the liquid nematic mesophase is characterised by an orientational order parameter. In nematics, contrary to the isotropic phase, orientations of molecules are not random. In the ground state, molecules are in average parallel to one direction indicated by the unit vector  $\mathbf{n}$  called director.

In the absence of fields and surfaces, the director can take any direction. The set of all possible directions that can be taken by the director can be represented by the unit sphere drawn in Figure 2e. In this case we would say the degeneracy space  $R_N$  of nematics is a two-dimensional sphere  $S^2$ . However, in non polar nematics, directions  $\mathbf{n}$  and  $-\mathbf{n}$  are equivalent so that degeneracy space  $R_N$  of the director is not the sphere  $S^2$  but the sphere  $S^2$  factored by the group  $Z_2$ :  $R_N = S^2 / Z_2$ . In other words, the states corresponding to antipodal pairs of points on the unit sphere are the same.

In the experiment described above, the director field  $\mathbf{n}(x, y, z)$  cannot be uniform because it must match the limit (anchoring) conditions:  $\mathbf{n} // z$  on glass slides and  $\mathbf{n} // y$  on the fiber surface.

As required, fields  $\mathbf{n}_I$  and  $\mathbf{n}_{II}$ , represented by black lines in the two regions labeled as "I" and "II" in Figure 2a, located respectively on the left and hand sides of the disclination loop, match these anchorings conditions. Let us stress that these drawings are not results of calculations; they were made by hand. Nevertheless, they are sufficient from topological point of view.

Let us remark now that these two fields are not identical: the field  $\mathbf{n}_I$  is the reflection of the field  $\mathbf{n}_{II}$  in the plane  $(x, z)$ . The issue is now: "can such two symmetrical fields  $\mathbf{n}_I$  and  $\mathbf{n}_{II}$  be connected in a continuous manner?". The answer given by the homotopy theory is: "No", there must be a singular line - the disclination - on which the direction of molecules (of the director  $\mathbf{n}$ ) is not well defined.

To get this answer, the homotopy theory proceeds as follows. Let us consider the rectangular closed trajectory ABCD with points A and D located on the nylon surface, while the points B and C are located on the glass slide. Segments AB and CD are located respectively on the left- and right-hand sides of the mirror plane  $(x, z)$ .

Let us examine now how the director field varies along this trajectory. In the point A, the director is parallel to the y axis:  $\mathbf{n}_A = (0, 1, 0)$ . As the segment AB lies on the fiber surface, all along it the director field keeps its orientation so that at the point B we have  $\mathbf{n}_B = (0, 1, 0)$ . Let us mark this orientation  $\mathbf{n}_{A,B} = (0, 1, 0)$  with a yellow small circle on the unity sphere drawn in Figure 2e. Along the segment BC, the director rotates around the x axis in the anticlockwise direction and varies from  $\mathbf{n}_B = (0, 1, 0)$  to  $\mathbf{n}_C = (0, 0, 1)$ . Along the segment CD located on the slide surface, the director conserves its vertical orientation so that we have  $\mathbf{n}_D = (0, 0, 1)$ . This orientation  $\mathbf{n}_{C,D} = (0, 0, 1)$  is labelled "CD" on the unit sphere in Figure 2e. Finally, along the last segment DA, the director rotates in anticlockwise direction around the axis x and arrives at A with orientation  $\mathbf{n}_A = (0, -1, 0)$ . This final orientation of the director is marked with the second small circle on the unit sphere in Figure 2e.

In conclusion, variation of the director along the closed trajectory ABCD in real space is represented on the unit sphere by the trajectory connecting the two antipodal points marked



with the yellow circles. In spite of the appearances, this trajectory is also closed because the directions  $\mathbf{n}$  and  $-\mathbf{n}$  are equivalent.

When the director field along the trajectory ABCD in real space surrounding the disclination is perturbed in a continuous manner, the corresponding trajectory on the unit sphere is perturbed too but it connects always two antipodal points. In general, the director field along all closed trajectories in real space surrounding the disclination line (such as the circular trajectory PP' in Figures 2b, c and d) is mapped on the unit sphere to trajectories connecting two antipodal points. As this property does not depend on the radius  $r$  of the circular trajectory, the director field must have a singularity in the limit  $r \rightarrow 0$ . This singularity is located at the captive disclination loop.

**Remark 1:** The captive disclination loop observed in experiments has thus a singular core. This type of disclination is called  $\pi$  because the director rotates by  $\pi$  on a circuit surrounding it.

**Remark 2:** If the fiber was replaced by a cylindrical volume of a nematic oriented in  $y$  direction, the disclination loop would collapse.

**Remark 3:** The disclination loop tethered on the polymer fiber cannot collapse because it is repelled by the fiber surface with the planar anchoring. One could say that it hovers at a constant altitude above the fiber surface.

### 3. Dislocations in cholesterics

In the second part of this memorial article devoted to Gerard Toulouse, we will focus on his another contribution to the field of topological defects in condensed matter published in the article untitled "Distortions with double topological character: the case of cholesterics" cosigned with Yves Bouligand, Valantin Poénaru, Bernard Derrida and Yves Pomeau.

This paper deals with the structure of Hopf links made of dislocations in cholesterics. Such objects have indeed a double topological character because, on one hand, dislocations are topological defects and, on the other hand, links (and knots) are archetypes of topological intricacies.

Our aim here is to present this pioneer work in light of recent experiments that allowed us to generate the Hopf links in cholesterics in a well controlled manner and to study in more details their features.

In 1978, the subject was initiated by interaction of Gerard Toulouse with Yves Bouligand, a biologist frequently visiting LPS in Orsay. Bouligand was interested initially by textures inside thin cuts of cuticles of insects and amphipods that he observed by means of an electronic microscope. After the outbreak of the interest in liquid crystals in France, Bouligand switched to observations, by means of a polarising microscope, of thin layers of cholesteric liquid crystals confined between glass plates. Like the chitin in cuticles, the molecules in cholesterics form in equilibrium helices of pitch  $p$  (Figure 3f). In samples with a very large pitch, Bouligand observed for the first time pairs of interlaced dislocations loops - the Hopf links [10].

For the sake of clarity, before discussion of these nested topological oddities, we need to introduce the concept of dislocations in cholesterics which is subtle enough on its own.

#### 3.1. Dislocations in Grandjean-Cano wedges

The wedge-shaped cholesteric layers (plane/plane in Figure 3a or cylinder/cylinder in Figure 3b) observed in the microscope (see Figures 3c and d) resemble topographic maps with patterns of contour lines which, in the case of cholesterics, indicate the variable number  $N$  of cholesteric pitches confined between the limit surfaces.

In the picture of Figure 3c, obtained with the plane/plane wedge geometry, we note the presence of two types of lines: **thin** and **thick** ones. The thin lines separate fields with  $N$  and

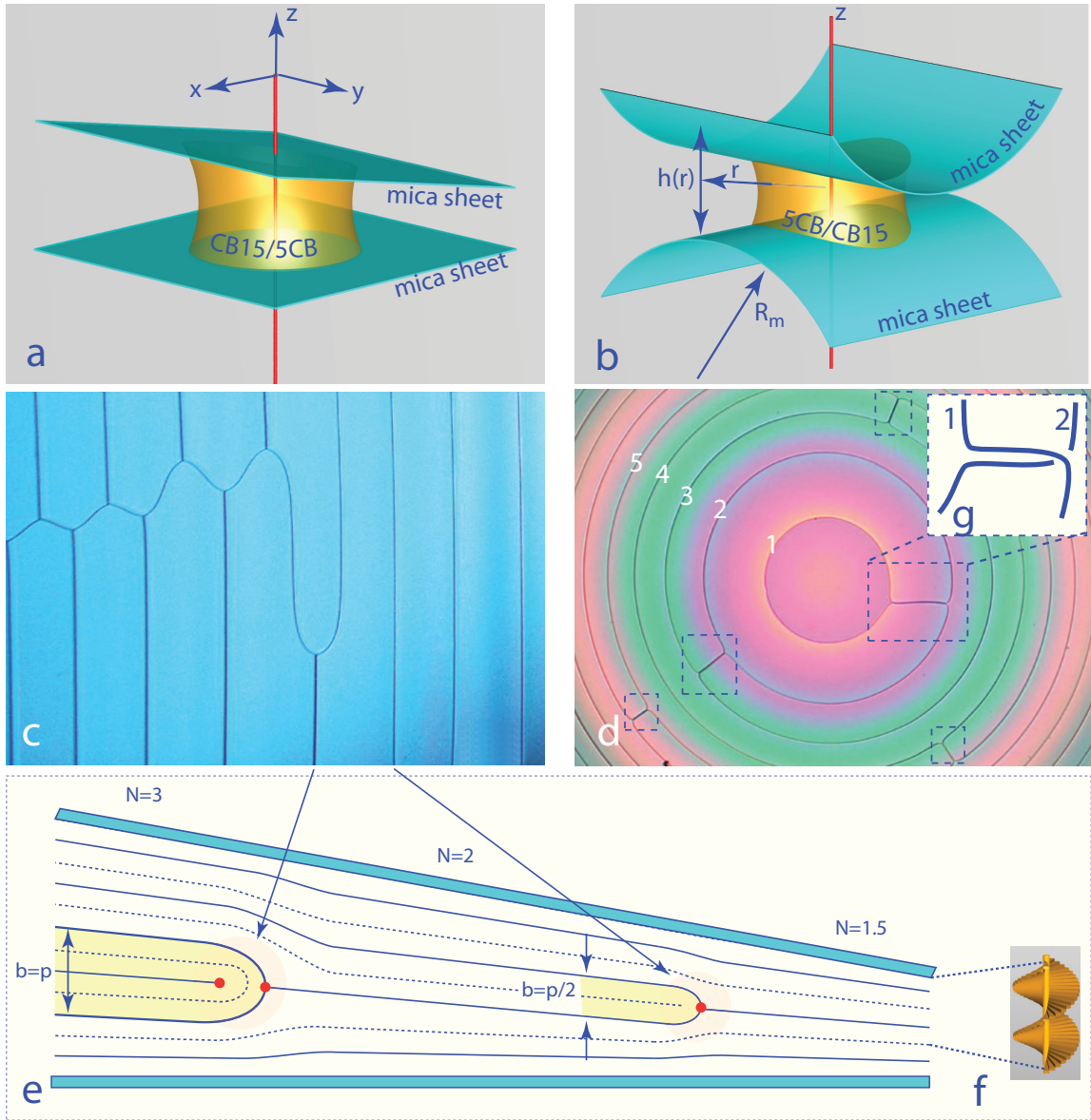


**Figure 3.** Dislocations in cholesterics confined between surfaces with planar anchoring. a) The plane/plane geometry of experiments of Bouligand [10]. b) The crossed cylinders geometry used in recent experiments [11, 12]. c) Dislocations' pattern in the plane/plane geometry. d) Dislocations' pattern in the cylinder/cylinder geometry. It corresponds to a multiply folded unknot. e) Cholesteric texture in the cross section of the dislocations' pattern in the plane/plane. f) Perspective view of the cholesteric helix. g) Two-level crossing of dislocations.

$N + 1/2$  of cholesteric pitches while the thick lines are frontiers between fields with  $N$  and  $N + 1$  pitches. In terms of the classification of topological defects, these two types of lines correspond to the two possible types of edge dislocations (see Figure 3c) with Burgers vectors  $b = p/2$  (thin lines) and  $b = p$  (thick lines). For this reason, thick lines in Figure 3c split into two thin lines.

### 3.2. Singular director field of the thin $b = p/2$ dislocation, homotopy theory

Since the pioneer work of Georges Friedel it is well known that there is no sharp phase transition between the nematic and cholesteric mesophases; when the pitch  $p$  of the cholesteric mesophase tends to infinity, it becomes identical with the nematic phase.

For this reason, dislocations in cholesterics can be seen also as disclinations [13]. Indeed, along a closed circuit ABCDA surrounding a thin ( $b = p/2$ ) dislocation, the director  $n$  rotates by  $\pi$  (see Figure 4c). Therefore, using the same arguments as those concerning the captive disclination loops, the director field of the thin dislocation must be singular.

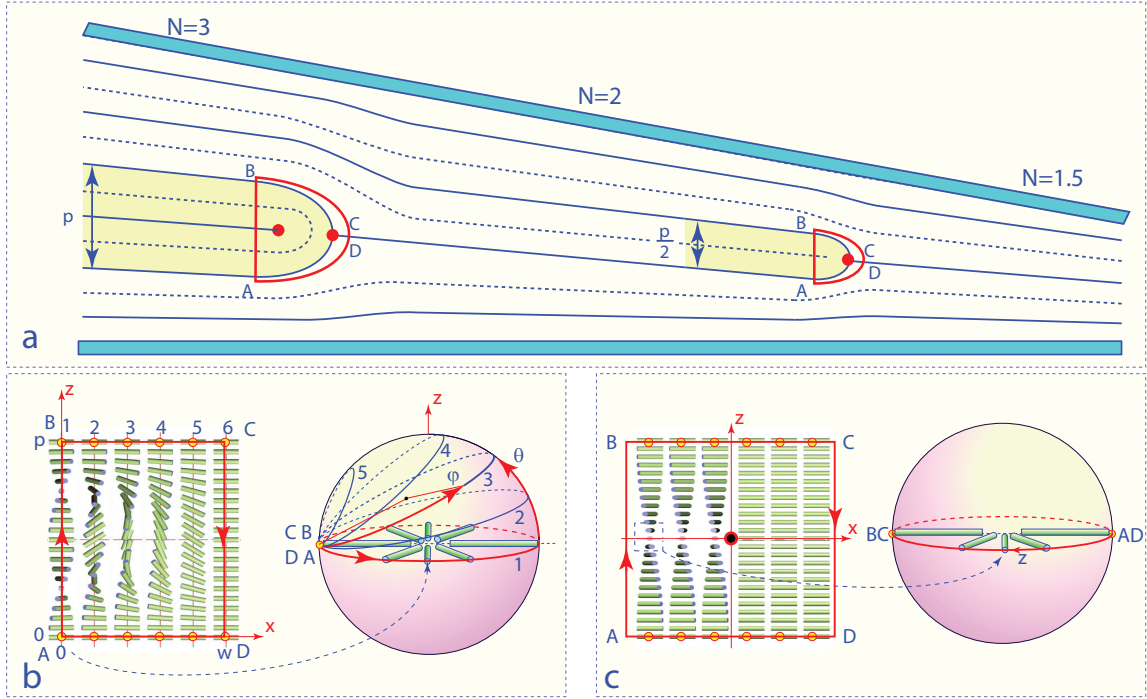


**Figure 4.** Dislocations in a cholesteric layer confined between two oblique planes. a) Definition of the **thick** and **thin** dislocations with Burgers vectors  $b = p$  and  $b = p/2$ . b) Non singular director field of the thick dislocation. c) Singular director field of the thin dislocation.

### 3.3. Nonsingular director field of the thick $b = p$ dislocation, homotopy theory

The director field of the "thick" ( $b = p$ ) dislocation in Figure 4a seems also to be singular in points marked with red circles. However, examination of this director field in terms of the homotopy theory leads to a different conclusion.

Let us consider the evolution of the director along the closed circuit ABCDA surrounding the  $b = p$  dislocation. Along the first segment AB, the director rotates by  $2\pi$  around the  $z$  axis but along the rest of the circuit it does not rotate at all. As the overall rotation of the director along the circuit ABCDA is  $2\pi$ , it is mapped onto the equator of the unit sphere (the degeneracy space of the director) where it is labelled "1" in Figure 4b.

In the same figure we show circles labeled from "2" to "5" which make the angle  $\theta$  with the equator and are tangent to it in the point labelled "A". The radii of such oblique circles vary as  $\cos(\theta)$  and shrink from 1 (the equator) to 0 (point A). If  $\varphi$  is the curvilinear coordinate (azimuthal



angle) that varies from 0 to  $2\pi$  along each of the oblique circles, then the director field can be expressed as:

$$\mathbf{n}(\theta, \varphi) = [-\cos^2(\theta) \cos(\varphi) - \sin^2(\theta), -\cos(\theta) \sin(\varphi), \cos(\theta) \sin(\theta)(1 - \cos(\varphi))] \quad (1)$$

Using the mapping rules  $\varphi = 2\pi z/p$  and  $\theta = (\pi/2)x/w$ , the director can be transplanted from the unit sphere in onto the rectangle  $[0 < z < p, 0 < x < w]$  in real space. The resulting director field  $\mathbf{n}(x, z)$  shown in Figure 4b is nonsingular. In conclusion thanks to the homotopy theory we arrived at the conclusion that, in contradistinction with the thin ( $b = p/2$ ) dislocation, the director field of the thick ( $b = p$ ) dislocation is nonsingular.

### 3.4. Kinks

Figures 5a and b show that the detailed texture of the director field of the thick ( $b = p$ ) dislocation depends on the mapping rules. The field in Figure 5b was obtained using  $\varphi = 2\pi(z - p/4)/p$  instead of  $\varphi = 2\pi z/p$  used in Figure 5a.

It can be shown that due to the elastic anisotropy of 5CB (nematic component of the chiral 5CB/CB15 cholesteric mixtures) the elastic energy per unit length  $T$  (in the  $y$  direction of the dislocation line) of the director field is larger in Figure 5b than in Figure 5a. In general, the

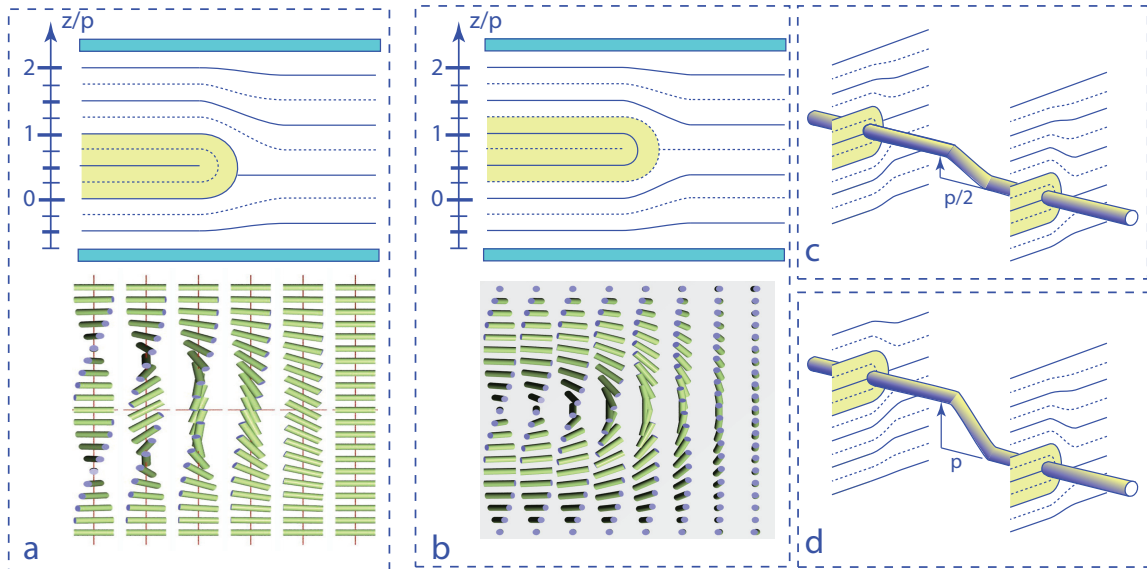


**Figure 5.** Kinks. a) Nonsingular director field of the thick ( $b = p$ ) dislocation obtained through the transplantation rules  $\varphi = 2\pi z/p$  and  $\theta = (\pi/2)x/w$  (see Figure 4b). b) Alternative director field obtained through the modified transplantation rule  $\varphi = 2\pi(z - p/4)/p$ . c) Kink of height  $p/2$ . d) Kink of height  $p$ .

tension  $T$  (energy per unit length) of the thick ( $b = p$ ) dislocation varies with its position  $z_D$  inside the cholesteric helix determined by the transplantation rule  $\varphi = 2\pi(z - z_D)/p$ . For  $z_D = 0, p/2, p, 3p/2, \dots$ ,  $T$  is minimal, while for  $z_D = p/4, 3p/4, 5p/4, \dots$  it is maximal. In the first approximation, we can write

$$T(z_D) = T_0 + \Delta T \sin^2(2\pi z_D/p) \quad (2)$$

The thick ( $b = p$ ) dislocation parallel to the  $y$  axis has therefore the tendency to stay locked in one of the available energy minima of  $T(z_D)$  occurring at  $z_D = 0, p/2, p, 3p/2, \dots$ . Transitions between different minima are then mediated by localised kinks such as those depicted in Figures 5c and 5d.

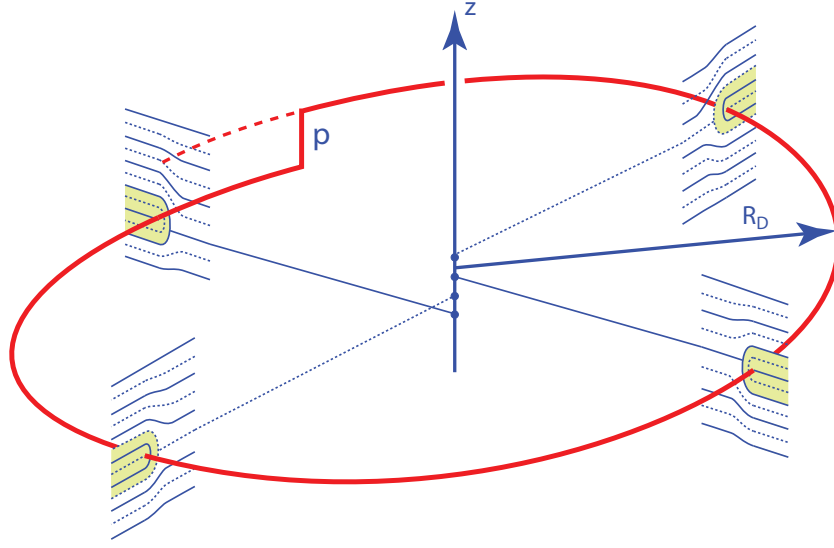


**Figure 6.** Helical shape of a dislocation loop in its ground state. Here it is buckled with one kink of height  $p$ .

### 3.5. Helical shape of dislocation loops

The tension  $T$  of the thick dislocation depends also on its orientation. The expression 2 is valid only for the dislocation parallel to the  $y$  axis. For different azimuthal directions of the dislocation making the angle  $\psi$  is with the  $y$  axis, the expression 2 has to be modified as follows

$$T(z_D, p\psi) = T_0 + \Delta T \sin^2(2\pi z_D / p - \psi) \quad (3)$$

As required, this new expression is invariant with respect to the symmetry operations of the cholesteric mesophase that associate rotation by the angle  $\psi$  with the translation  $\Delta z = p\psi / (2\pi)$ . For example, the minimum of the tension given by equation 3

$$T(z_D, p\psi) = T_0 \quad (4)$$

occurs for

$$z_D = p \frac{\psi}{2\pi} \quad (5)$$

This condition is satisfied in particular when the dislocation takes the helicoidal shape given by

$$x_D = R_D \cos(\psi) \quad (6)$$

$$y_D = R_D \sin(\psi) \quad (7)$$

$$z_D = p \frac{\psi}{2\pi} \quad (8)$$

where  $R_D$  is the radius of the helix (see Figure 6).

In conclusion, a dislocation loop in its ground state cannot be flat; it must take a helicoidal shape buckled with one kink of height  $p$  or with two kinks of height  $p/2$ .

### 3.6. Bridge-like crossings of dislocations

The relationship  $z_D = p\psi / (2\pi)$  between the orientation of a dislocation (expressed by the azimuthal angle  $\psi$  and its  $z$  position inside the cholesteric helix) has another important consequence concerning crossings of dislocations such as the one in Figure 3g discussed previously.

The scheme of the crossings depicted in Figure 3g shows that it is bridge-like because the two dislocations crossing each other have different orientations  $\psi$  so that their  $z$  position cannot be same.

Let us stress that systems of dislocation lines with the bridge-like crossings remind mathematicians and theorists of knots and links represented by their shadow-like projections on a plane. (In the case of Figure 3a, all visible crossings belong to one multiply folded unknot.) They would ask: "do these crossings belong to unknots or to knots or links?".

#### 4. Discovery of the Hopf link made of dislocations

This issue was initiated by Bouligand in one of his papers on textures and defects in cholesterics [10], beautifully illustrated with pictures taken with a microscope and with his own hand-made drawings. In his paper, Bouligand reports on the presence of pairs of interlaced dislocation loops such the one shown in Figure 7a.

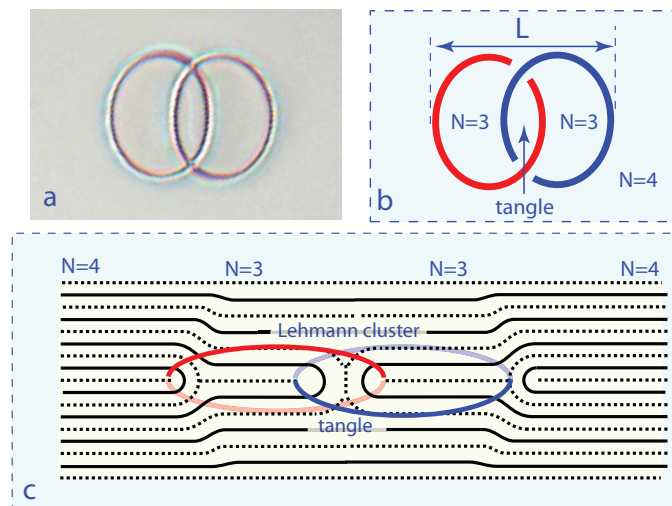


**Figure 7.** The "double anneau" texture made of dislocations discussed in references [10] and [14]. a) Microscopic picture obtained in a recent experiment with a cholesteric sample (5CB/CB15) confined in the crossed cylinders geometry. b) Geometry of the interlaced dislocation loops observed from above. c) Side view of the cholesteric texture.

The discovery of this texture, called by Bouligand "double anneau", inspired indeed theorists and lead to publication in 1978 of the article untitled "Distortions with double topological character [14]: the case of cholesterics" that Bouligand cosigned with B. Derrida, V. Poénaru, Y. Pomeau and Gerard Toulouse. As stressed in the title, the "double anneau" configuration has a **double topological character** :

- (1) dislocations themselves are linear topological defects of the cholesteric order parameter,
- (2) simultaneously, the interlaced rings have the nontrivial topology of the Hopf link.

Surprisingly, to our knowledge, the observation by Bouligand of the "double anneau" texture was not confirmed for decades in spite of the fact that patterns of dislocations of cholesteric liquid crystals called commonly "oily streaks" were extensively studied and displayed in articles and books. As a possible explanation of this anomaly we could invoke the fact that the articles of Bouligand were written in French so that the findings reported by Bouligand remained wrongfully in shadow.

## 5. Distortions with the double topological character, new experiments

### 5.1. Setup

Here, we will report on experiments performed recently with the setup depicted schematically in Figure 3b, which was built with the purpose to illustrate with color pictures of dislocations an article written in honor of Maurice Kleman [12] who passed away in 2021, two years before Gerard Toulouse. In this setup (see Figure 3b), a cholesteric droplet is maintained by capillarity between two identical crossed cylindrical mica sheets. Using the mica sheets instead of the glass slides has three advantages:

- (1) surfaces of freshly cleaved mica sheets are perfectly clean
- (2) their atomic crystalline structure is anisotropic and has the suitable property of orienting the molecules of the cholesteric of in one direction parallel to the mica surface
- (3) thin mica sheets being very flexible are easy to bend

As the thickness of the cylinder/cylinder gap varies as :

$$h(x, y) \approx h_{min} + \frac{x^2 + y^2}{2R_m} = h_{min} + \frac{r^2}{2R_m} \quad (9)$$

where  $R_m$  is the radius of curvature of the mica sheets, dislocations are expected to form in equilibrium a target-like pattern made of concentric circles with radii  $r_N$  satisfying the equation

$$Np + 1/2 = h_{min} + \frac{r_N^2}{2R_m} \quad (10)$$

where  $N$  is an integer.

### 5.2. Nucleation of folded unknots

With the aim to test this prediction we made a detailed study of nucleation of dislocation loops driven by a compressive strain of cholesteric layers squeezed between the cylindrical mica sheets. We expected that a slow compression of the gap (reduction of the minimal thickness  $h_{min}$ ) should result in nucleation, one after another, of circular individual concentric dislocation loops with decreasing index  $N$  forming together the target-like pattern.

Surprisingly, when the initial thickness  $h_{min}$  of the gap expressed in units of  $p$ ,  $N = h_{min}/p$ , was for example of the order of 10, several dislocation loops were nucleated in one burst and they were not individual but interconnected by crossings into folded "superloops". An example of such a superloop is shown in Figure 3d) where five loops labeled from 1 to 5 are interconnected by crossings such as the one between the loops 1 and 2 represented in the insert 3g.

For the sake of simplicity, let us consider the second example of the folded superloops shown in Figure 8a and a'. Here, two superloops were nucleated simultaneously. They are made of two loops connected by one crossing. From topological point of view they are folded (twisted) unknots. Theoretically, the crossing could be removed by the Reidemeister move "untwist" so that the folded unknots would be transformed into a trivial circular unknots. However, in practice, the "untwist" move is energetically forbidden in the crossed cylinders geometry so that the folded unknot configuration is stable as long as the minimal thickness remains small enough.

### 5.3. Coalescence of two folded unknots into the Hopf link

The second surprise came when, during their expansion, the two folded unknots collided (see Figures 8a and a'). First, the external dislocations loops of the two unknots coalesced (merged)

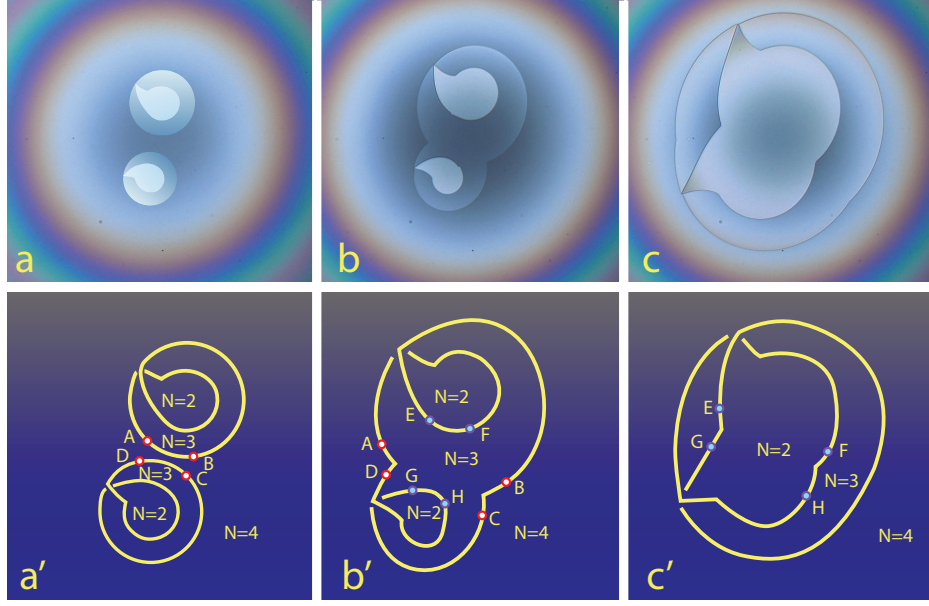


**Figure 8.** Genesis of the Hopf link. a-a') Nucleation of two folded unknots. b-b') Coalescence of the external loops of the two colliding folded unknots. c-c') Coalescence of the internal loops of the folded unknots.

(see Figures 8b and b'). The coalescence can be seen as a rewiring process resulting from the collision of the AB and CD segments:  $AB + CD \Rightarrow AC + BD$ . As a result, the two folded unknots became connected into one unknot folded twice.

Finally, the expansion of the two internal folds lead to a new collision followed by the coalescence of the folds:  $EF + GH \Rightarrow EG + FH$ . The result of the two successive collision-coalescence events is shown in Figures 8c and c': the crossings of the two unknots are gathered together into the elementary Hopf link.

Let us stress that this method of producing the Hopf link is reproducible because nucleation of the folded unknots is heterogenous and occurs always at the same points - locations of the nucleation centres.

#### 5.4. Instability of the symmetrical configuration of the Hopf link

After the first identification of the Bouligand's "double anneau" made of interlaced dislocation loops in our samples with large pitches ( $p \approx 40\mu m$ ) (see Figure 7a), we reexamined videos recorded in previous experiments and have found that in fact the Hopf links were occurring quite frequently in them. The reason for which we did not identified them previously is the following.

The Hopf link is usually represented as two interlaced loops of the same size (see Figure 7b) even if from topological point of view the size of the interlaced loops does not matter. In practice, such a symmetrical configuration is energetically unstable and evolves in two different ways. Let us suppose that (1) the Hopf link is located in the center of the crossed cylinders gap where the thickness  $h(x,y)$  is minimal and (2) the sizes of the interlaced rings are the same  $r \approx L/2$ . It can be shown that due to the tension  $T$  of dislocations (energy par unit length), there exist the critical radius  $r_{Nc}$  (see Figure 7a)

$$r_{Nc} = p \frac{\tilde{T}}{h_N / h_{min} - 1} \quad (11)$$

with  $\tilde{T} = T/(4\pi K_{22})$  and  $h_N = pN + 1/2$ , defining two different cases:



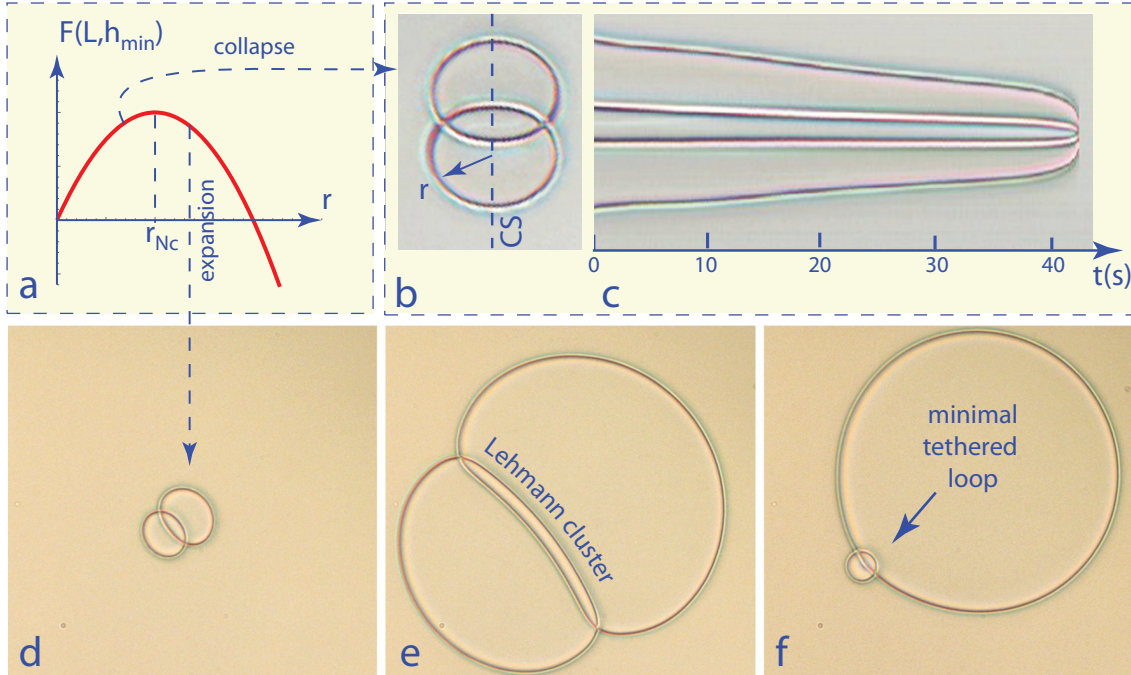


**Figure 9.** Instability of the Hopf link. a) Variation of the energy of dislocation loops with their radius  $r$ . b) Symmetrical configuration of the Hopf link. In this picture, its size is smaller than the critical one  $r_{Nc}$  given by equation 11. c) Spatio-temporal cross section showing the shrinking and the final the collapse of the Hopf link. d) Almost symmetrical configuration of the Hopf link. e) When  $r < r_{Nc}$  the interlaced loops expand until they reach their equilibrium size. They remain associated by the dislocations' pair known as the Lehmann cluster. f) On a longer time scale, the length of the Lehmann cluster is reduced for energetical reasons so that the smaller dislocation loop shrinks until reaches its minimal size. One obtains an asymmetric configuration, called **necklace**, of the minimal loop tethered on the large loop.

- (1) for  $r < r_{Nc}$ , the interlaced loops will shrink and the Hopf link will collapse as it is shown in Figures 9b and c,
- (2) for  $r > r_{Nc}$  (Figure 9d), the interlaced loops will expand into the configuration shown in Figure 9e in which they remain associated by the dislocations' pair known as the Lehmann cluster. The Lehmann cluster has some energy per unit length of the order of  $2T$  so that on a longer time scale it shrinks until the smaller dislocation loop reaches its minimal size (see Figure 9f). The asymmetric configuration of the **minimal loop tethered on the larger cargo loop** will be called below **necklace**.

In conclusion, the symmetrical configuration of the Hopf link is unstable and therefore exceptional. The asymmetric necklace configuration is therefore the most frequent. However, as the diameter of the minimal loop is of the order of  $p$ , in samples with very short pitches  $p \approx 1\mu m$ , the minimal tethered loops can be easily confused with impurities trapped by the larger cargo loop.

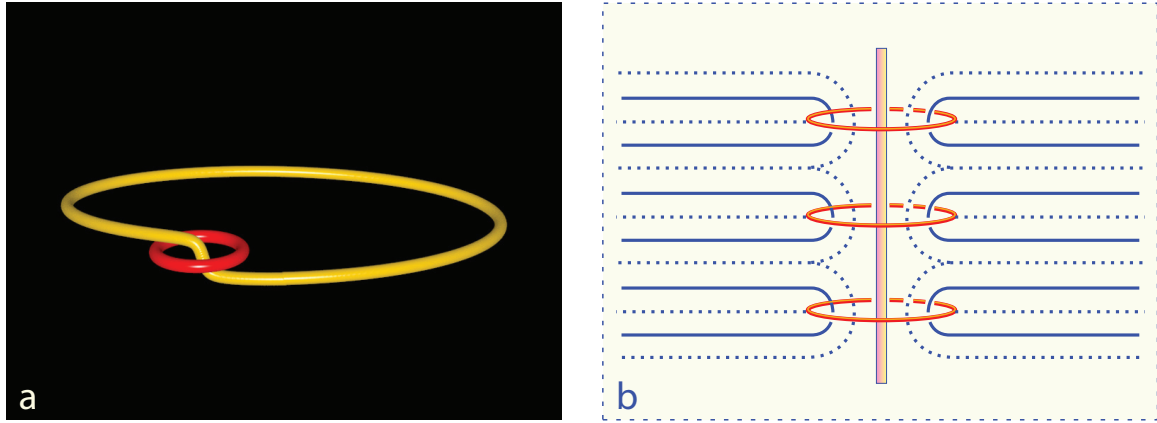


**Figure 10.** Necklace configurations of the Hopf link. a) One minimal loop tethered on the kink of the large cargo loop. b) Periodic system of minimal loops tethered on a straight screw dislocation imagined by Rault [15].

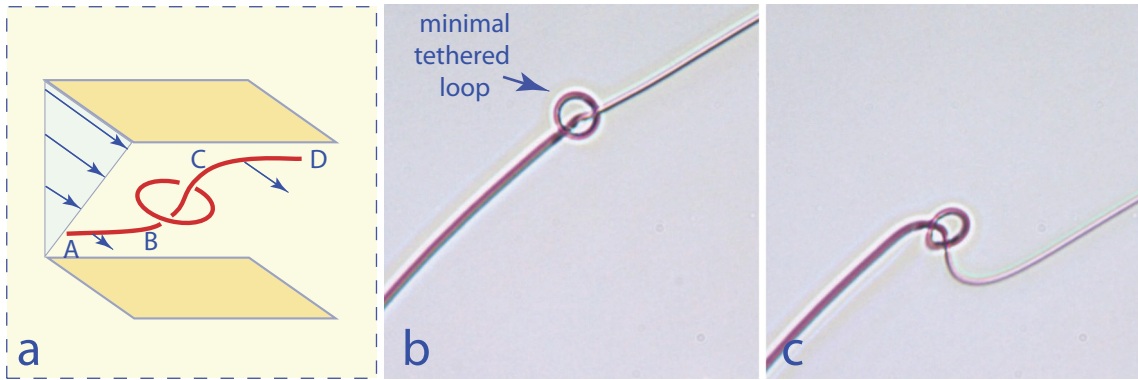


**Figure 11.** Robustness of the Hopf link in its necklace configuration with respect to a shear deformation. a) Geometry of the experiment. b-c) Deformation of the necklace unveils its three dimensional structure.

### 5.5. Robustness of the Hopf link, in its necklace configuration, with respect to a shear deformation

In ref. [14], the Hopf link made of the dislocations with the Burgers vector  $b = p$  (called "J" in ref. [14]) has been termed "topological atom" because the interlaced dislocation loops cannot be easily unlinked without a local destruction of the cholesteric order. This kind of the robustness of the Hopf link appears in the experiment depicted in Figures 11 where a shear flow driven by the horizontal motion of the upper mica sheet is applied to the sample. Viscous forces acting on the minimal and large loops, deforms them strongly. In spite of that, no matter how large is this deformation, the minimal loop remains tethered on the large one.

By the way, let us stress that this experiment unveils the geometry of the cargo loop in the vicinity of the minimal loop. Let  $z = 0$  be the level of the minimal loop. The cargo loop is made of two segments AB and CD located at different levels,  $z_{AB} = -p/2$  and  $z_{CD} = p/2$ , and connected by a kink of height  $z_{AB} - z_{CD} = p$ . In first approximation, the kink can be seen as a vertical segment BC of the cargo loop passing through the center of the minimal loop.

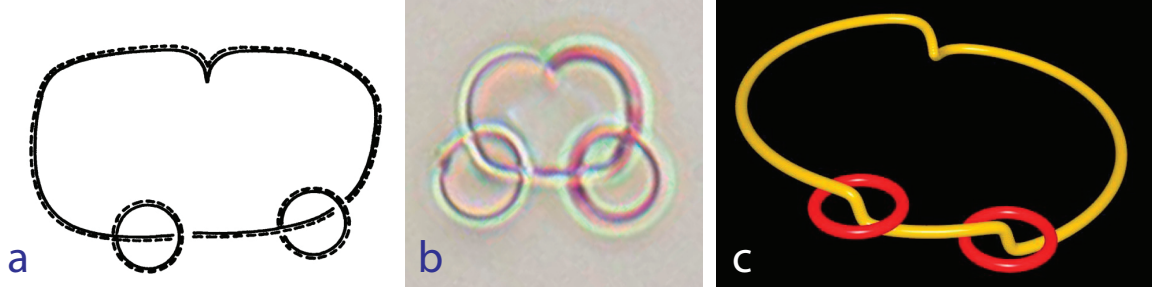


**Figure 12.** "The triple ring structure" predicted in ref. [14]. a) Reproduction of the Figure 1 from ref. [14]. b) The three components Hopf link observed in our experiments. c) Perspective view showing three kinks on the cargo loop carrying the two minimal loops.

### 5.6. *Necklace configuration of the Hopf link*

The large cargo loop of the necklace configuration has, as expected, the helical shape and is buckled with the kink of height  $p$  (see Figure 10a). The minimal loop, tethered on this kink of cargo loop, is flat (see Figure 10a)) because the kink can be seen as a short segment of a nonsingular vertical screw dislocation with the Burgers vector  $b = p$ . This configuration of flat edge dislocation loops tethered on a vertical screw dislocation has been imagined and discussed for the first time by Rault [7, 15].

### 5.7. *Ubiquity of the Hopf links, Hopf necklaces*

After the first identification of the Hopf link in its necklace configuration we have found that several minimal loops can be tethered on one cargo loop. In particular, we observed (see Figure 12b) the configuration of two minimal loops tethered on the cargo loop represented in Figure 12a which was conjectured in the article of Bouligand et al. [14]. The perspective view in Figure 12c allows to identify three kinks on the cargo loop. The two minimal loops are tethered on kinks of height  $\Delta z_1 = \Delta z_2 = -p$ . The third kink, called cuspidal in ref. [14] has opposite sign :  $\Delta z_c = +p$ .

The total change of the height  $z$  due to these three kinks encountered on an anticlockwise circuit along the cargo loop is thus  $\Delta z_1 + \Delta z_2 + \Delta z_c = -p$ . Let us remind that, as discussed in Section 3.5, the change of the azimuthal direction of the cargo loop by  $\Delta\psi = 2\pi$  results in the change of height of  $\Delta z_{loop} = +p$ .

After taking into account all contributions we have

$$\Delta z_1 + \Delta z_2 + \Delta z_c + \Delta z_{loop} = 0 \quad (12)$$

This conservation law written in a different form was used by Bouligand et al. [14] for prediction of the "triple ring" configuration.

### 5.8. *Stability of the Hopf necklaces*

In the second example of the Hopf necklaces shown in Figure 13 we can identify three minimal loops tethered on the  $\Delta z_k = -p$  kinks of the cargo loop. Beside them, there are several cuspidal points corresponding to  $\pm p/2$  kinks. The cuspidal kinks can move along the cargo loop and assemble into kinks of height  $\Delta z_c = p$ . Such free kinks of height  $\Delta z_c = p$  are enemies of the minimal loops: the minimal loops are incorporated into the cargo loop after their encounters with the kinks. We postpone a more detailed discussion of this issue to another paper.

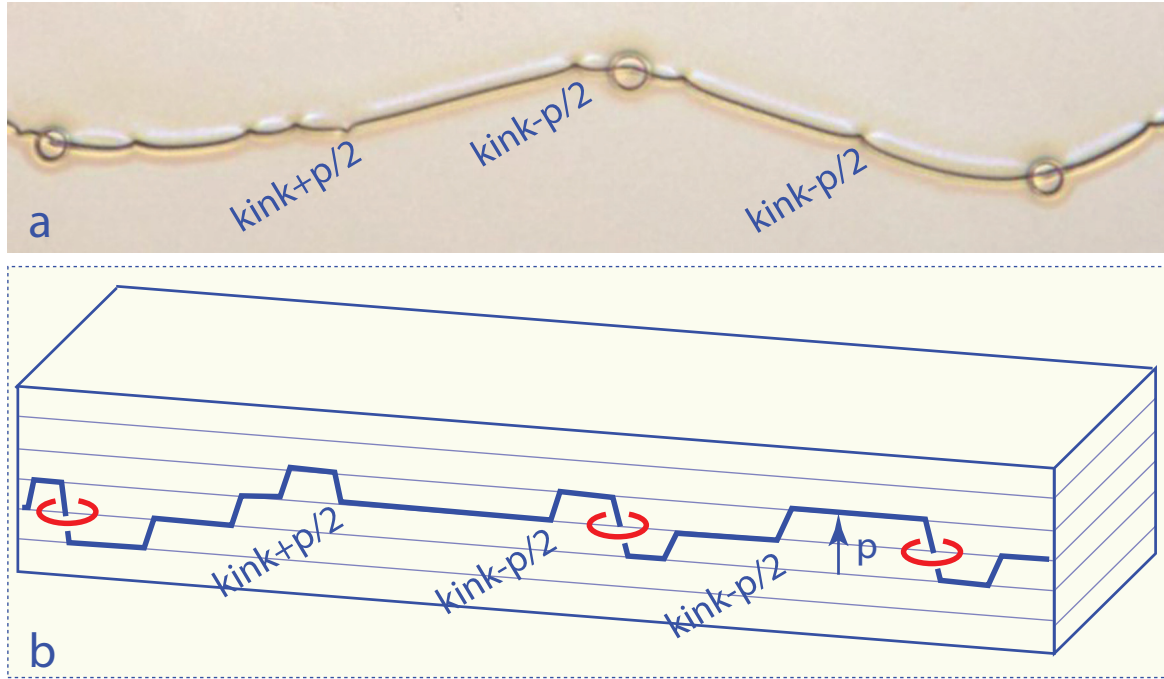


**Figure 13.** Segment of a Hopf necklace with three minimal loops tethered on a cargo dislocation containing several  $\pm p$  kinks. a) Vue in a microscope. b) Perspective view.

## 6. Conclusions

"Long temps me fut nécessaire pour comprendre les tenants et les aboutissants de ma vocation, singulière".

The sound of this sentence, written by Gérard Toulouse at the beginning of a short text untitled "Le sens d'une exploration" and published in the book "Le goût de la science" [16], unveils the subtle and engaging soul of Gérard.

As already said in the Introduction, one of the authors of the present article (P.P.), as a PhD student, had the chance to listen to his wonderful lectures on topological aspects of physics in Laboratoire de Physique des Solides in Orsay. Many years later, as a lecturer at Ecole Normale rue Lhomond, he met Gérard again who, at the end of this encounter, generously offered him the book mentioned above.

Today, another classical text comes on mind: "*Exegi monumentum aere perennius...Non omnis moriar...*". The legacy of Gérard contains written contributions which like those of Horace, were, are and will be quoted. However, among the traces left by Gérard even more important are those that are *invisible to the eye*: his impacts on minds. The present article reporting on recent experiments with topological defects and with knots and links is like a plant grown from a seed sown by Gérard many years ago.

## References

- [1] G. Toulouse, M. Kleman, "Principles of a classification of defects in ordered media", *Journal de Physique Lettres* **37** (1976), p. L-149.
- [2] J. Friedel, *Dislocations*, 1 ed., Pergamon Press, Oxford, 1964.
- [3] P. Pieranski, "Dislocations and other topological oddities", *Comptes Rendus de l'Académie des Sciences* **17** (2016), p. 242-263.

- [4] P.-G. de Gennes, *Superconductivity of metals and alloys*, 1 ed., Benjamin, New York, Amsterdam, 1964.
- [5] P. Pieranski, "Pierre-Gilles de Gennes: beautiful and mysterious liquid crystals", *Comptes Rendus de l'Académie des Sciences* **20** (2019), p. 756-769.
- [6] M. Kleman, O. Lavrentovich, *Soft matter physics: an introduction*, 1 ed., Springer, New York, 2001.
- [7] M. Kurik, O. Lavrentovich, "Defects in liquid crystals: homotopy and experimental studies", *Usp. Fiz. Nauk* **154** (1988), p. 381-431.
- [8] I. Smalyukh, "Review: knots and other new topological effects in liquid crystals and colloids", *Rep. Prog. Phys.* **83** (2020), p. 1-46.
- [9] M. Dazza, L. Cabeca, S. Copar, M. H. Godinho, P. Pieranski, "Action of fields on captive disclination loops", *EPJE* **40** (2017), p. 28.
- [10] Y. Bouligand, "Recherches sur les textures des états mésomorphes. 6- Dislocations coin et signification des cloisons de Grandjean-Cano dans les cholestériques", *Journal de Physique* **35** (1974), p. 959-981.
- [11] P. Pieranski, M. H. Godinho, "Fertile metastability", *Liquid Crystals* (2023), p. 1-16.
- [12] P. Pieranski, "Cholesteric dislocations in mica wedges", *Liquid Crystals Reviews* **9** (2022), p. 65-92.
- [13] M. Kleman, J. Friedel, "Lignes de dislocations dans les cholestériques", *J. de Phys.* **30** (1969), p. C4-43-C4-53.
- [14] Y. Bouligand, B. Derrida, V. Poénaru, Y. Pomeau, G. Toulouse, "Distorsions with double topological character: the case of cholesterics", *Journal de Physique* **39** (1978), p. 863-867.
- [15] J. Rault, "Dislocation  $\chi$  dans les cholesteriques: II. Modeles des dislocations  $\chi$ ", *Philos. Mag.* **29** (1974), p. 621-640.
- [16] G. Toulouse, "*Sens d'une exploration*" dans *Le goût de la science*, 1 ed., Alvik, Paris, 2005.